

# Synthesis of Amide-Based Surfactant Inhibitor for Carbon Steel Corrosion Protection Electrochemical Analysis

Xiaoping Wang\*, Hanbin Xiao

School of Logistics Engineering, Wuhan University of Technology, 430063, Wuhan, China

\*E-mail: [xiaopingwang\\_zzz@foxmail.com](mailto:xiaopingwang_zzz@foxmail.com)

Received: 6 October 2016 / Accepted: 18 November 2016 / Published: 12 December 2016

---

In this paper, a variety of amide-based cationic surfactants were synthesized through the chemical route. Then, the properties of the as-prepared surfactants, such as the surface tension, the minimum surface area, the maximum surface excess and the critical micelle concentration, were investigated. The <sup>1</sup>H NMR and FTIR spectra was recorded to determine their structures. The corrosion inhibition capacity of the as-synthesized amide-based surfactants was evaluated on the carbon steel, where the polarization, weight loss and electrochemical impedance experiments were performed. It was demonstrated that the surfactants were immobilized well on the surface of the carbon steel, which could be elaborated with Langmuir adsorption isotherm. The influences of various parameters further were investigated and discussed.

---

**Keywords:** Amide-based cationic surfactant; Corrosion; Carbon steel; Chemical structure; Surface tension

## 1. INTRODUCTION

In numerous industrial manufacture, the acid mediums are applied to remove the undesirable substances or the products of corrosion in the metallic materials. Among the acidic solutions, sulfuric and hydrochloric acids are the most widespread [1]. However, metallic corrosion takes place during the process, which is the deterioration of the metals or the alloys through the electrochemical reaction accompanied with diverse influences. For example, serious economic losses are induced by this corrosion in several industrial areas all over the world [2]. Thus, to prevent the erosion as well as reduce the usage of acid, organic corrosion inhibitors are into the system, where majority of the inhibitors contain N, O and S heteroatoms in their structures. Especially, between the surface of the metal and the molecules of the inhibitor, electrostatic interaction will take place through these

heteroatoms contained in the structure of the inhibitor. Besides, the possible centres of adsorption could be provided by these heteroatoms for the chemical adsorption. Hence, to develop new compounds for corrosion inhibition is promising and must be continued despite that numerous organic compounds have been synthesized as inhibitors [3]. Especially for the petroleum industry, developing inhibitors is of great importance to prevent the corrosion effect induced by 1.5 M HCl. For instance, organic compounds, which contain the electronegative functional groups like hydroxyl group, exhibited remarkable performance of corrosion inhibition towards numerous metals and alloys [4-6]. In general, the inhibitors are adsorbed on the surface of the target by the interaction between the functional group and the surface, which will further hinder the target surface from directly interacting with the erosive materials. Hence, the corrosion rate will be reduced, resulting in the extension of the life of the target. Besides, some organic inhibitors containing nitrogen-based groups were developed and found to exhibit intriguing performance of corrosion inhibition.

By far, amide-based organic substances have been extensively applied in industry, where one of the most essential applications was serving as corrosion inhibitor. According to the literature, numerous researches have been performed for the corrosion inhibition of the metals or the alloys in the acidic medias with the amide-based organics substances containing long carbon chains [7-12]. Recently, the research on the corrosion inhibitor consisting of the cationic-based surfactant has become significant crucial, where new compounds such as the cationic surfactants containing amide-based group have been reported to exhibit the characteristic of the corrosion inhibitor [13-17].

Synthetic aliphatic acids and their derivatives have been widely applied, primarily as the industrial raw materials. Besides, the potential applications of these materials involve the chemicals in oil-field, where the substances with long chains are employed widely as the corrosion inhibitors in the oil industry. Serious economic damage is caused by the industrial corrosion due to the disruption of the equipment made of metal or alloy and the deterioration of the industrial products. The cationic-type surfactants have been demonstrated to be the excellent inhibitors in definite acidic medium [18]. The hydrophobic protective layer consisting of the molecules of these surfactants generated on the metal surface efficiently prevent the corrosion effect from the corrosive media. However, for several erosive systems, particularly the water-oil liquid system, the surfactants require to contain hydrophilic groups in their structures to act as the effective corrosion inhibitors, where these groups influence their solubility so that they can be more soluble or dispersible in such mediums.

Herein, we synthesized various organic cationic surfactants containing the amide functional group. Furthermore, the corrosion inhibition capacity of the as-synthesized surfactants was investigated in acidic aqueous solution, where diverse chemical and electrochemical experiments were conducted.

## 2. EXPERIMENTS

### 2.1. Materials

All the reagents and solvents were commercially available (Merck and Fluka Chemie) and used as received without any purification unless stated otherwise. A Buchi melting point apparatus was

employed to measure the melting points. Thermo Nicolet FTIR spectrometer was used to collect the IR spectra. A Varian Mercury Plus spectrometer was utilized to record the  $^1\text{H}$  NMR spectra in  $\text{CDCl}_3$ , where TMS was used as the internal standard. A contact angle measurement system was employed to measure the static water contact angle at room temperature. Tensiometer (K 100 mode) was used to perform the measurements of the surface tension of the synthetic surfactant inhibitors. Besides, SEM (JEOL 5400) was used to analyze the surface EDX of the carbon steel samples, where the analytical software was utilized to normalize the peak noise of the spectra.

## 2.2. Synthesis of Compounds

*2-Chloro-N-alkylacetamides.* The syntheses of 2-chloro-N-octyl (CN-1) and -dodecyl (CN-2) were carried out under the similar conditions as described in the previous literatures [19, 20].

*N-Alkyl-2-(4-formyl-2-methoxyphenoxy)acetamides (NAF).* Vanillin (1 equivalent) and  $\text{K}_2\text{CO}_3$  (2 equivalent) were added into a round-bottom flask (100 mL). Then the solvent DMF (25 mL) was added into the flask. After a few minutes, the corresponding 2-chloro-N-alkylacetamide was added to the mixture. Subsequently, the mixture was stirred and refluxed overnight at 65-70 °C. Then, the mixture was extracted by  $\text{CHCl}_3$  after the addition of the cold water. The organic phase was collected and dried with  $\text{Na}_2\text{SO}_4$ . Then the solvent was removed under reduced pressure by a rotary evaporator. At last, the residue was crystallized in THF/petroleum ether.

*N-Alkyl-2-[4-(hydroxymethyl)-2-methoxyphenoxy]acetamides (NAH).* In a round-bottom flask (100 mL), NAF (1 equivalent) was dissolved in ethanol (15 mL) and cooled to 0-5 °C. Then  $\text{NaBH}_4$  (2 equivalent) was added in portions. The reaction mixture was warmed to room temperature and stirred for 3 h. Then the solvent was removed under reduced pressure. The residue was added into the cold water and filtered under vacuum to obtain the white solid. As last, the solid was dried at room temperature and crystallized in methanol/water.

## 2.3. Chemical composition of tested carbon steel

In this paper, the employed carbon steel was X-65 type. The chemical composition of the X-65 type carbon steel was illustrated in Table 1. To study the weight loss, the carbon steel which was in the form of regular edged cuboid was sliced. However, in regard of the polarization and electrochemical investigations, the carbon steel of small piece was first placed into the epoxy resin and polished, which further was employed as an electrode with a surface area of 1  $\text{cm}^2$ .

**Table 1.** The chemical composition of X-65 carbon steel.

Element	C	Mn	Si	P	S	Ni	Cr	Mo	V	Cu	Al
Content (w/w)	0.12	1.44	0.30	0.01	0.05	0.04	0.03	0.01	0.002	0.02	0.04

#### 2.4. Weight loss measurements

The weight loss measurements were performed with the carbon steel samples with a size of 5 cm × 2 cm × 0.4 cm. The weight loss was recorded at various immersion times of the carbon steel samples in HCl with a concentration of 1.5 M in the presence of the surfactant inhibitors, whereas the control experiment was carried out in the absence of the surfactant inhibitors under the same conditions. The corrosion product generated on the surface of the carbon steel was rinsed with water. At last, the weight of the remaining carbon steel was measured and compared to that of the carbon steel before experiment.

#### 2.5. Electrochemical characterization

The electrochemical measurements were carried out on a CHI 660 electrochemical workstation with the traditional three-electrodes system, where the carbon steel sample acted as the working electrode, a platinum was employed as the counter electrode and the saturated calomel electrode served as the reference electrode. Besides, Tacussel corrosion analysis software was employed. The steady state of the circuit potential was established through the pre-immersion of the working electrode for 1 h. The potentiodynamic polarization curves were used to evaluate the polarization performance of the carbon steel under 1 mV/s. The carbon steel which was immersed in acidic water in the presence and absence of the diverse surfactant inhibitors was analyzed with electrochemical impedance spectroscopy.

### 3. RESULTS AND DISCUSSION

Several cationic surfactants were prepared, which could serve as the potential corrosion inhibitors for the low-carbon steel in acidic medium. The starting materials employed in the synthesis of these surfactants were easy to be synthesized. To prepare the starting compounds, various amines with long chains was treated with chloroacetyl chloride to obtain the corresponding 2-chloro-N-alkylacetamides, which then reacted with vanillin to obtain these compounds. After that, these compounds were reduced in a proper solvent by NaBH<sub>4</sub>. Then, the obtained products were treated with SOCl<sub>2</sub>.

The IR spectrum of CN-1 exhibited the adsorption bands locating at 3217, 3031 and 1669 cm<sup>-1</sup>, which were ascribed to the amide -NH group, the aromatic =C-H stretching and the amide C=O group, respectively. For NAF, three characteristic adsorption bands at 3331, 1768 and 1678 cm<sup>-1</sup> were observed in the IR spectrum, which were attributed to the amide -NH group, the ketone C=O stretching and the amide C=O group, respectively. In the case of NAH, the adsorption bands in the IR spectra were found to locate at 3419, 3131 and 1669 cm<sup>-1</sup>, which could be ascribed to the amide -NH group, the pyridine =C-H stretching and the amide C=O group.

In the <sup>1</sup>H NMR spectrum of CN-1, a singlet at δ 4.88 ppm was ascribed to the protons of the the ArCH<sub>2</sub>-N<sup>+</sup>, a quadruplet at δ 3.45 ppm was attributed to the protons of the -N<sup>+</sup>(CH<sub>2</sub>CH<sub>3</sub>)<sub>3</sub> and a

triplet at  $\delta$  1.45 ppm belonged to the methyl protons in the  $-\text{N}^+(\text{CH}_2\text{CH}_3)_3$  group. For CN-2, two triplets at  $\delta$  6.26, 4.48 ppm and a quintet at  $\delta$  1.51 were observed in the  $^1\text{H}$  NMR spectrum, which were attributed to the protons of the  $\text{ArCH}_2\text{-Py}^+$ , the protons of the  $-\text{CH}_2\text{O}$  and the methylene protons of the  $-\text{CH}_2\text{CH}_2\text{CH}_2\text{NH}$  group, respectively. However, the  $^1\text{H}$  NMR spectrum of NAF displayed four main peaks including two singlets at  $\delta$  5.51, 4.52 ppm, a quintet at  $\delta$  3.86 and a triplet at  $\delta$  1.44, which belonged to the protons of the  $\text{O=CCH}_2\text{-N}^+$ , the protons of the  $-\text{CH}_2\text{OAr}$ , the protons of the  $-\text{N}^+(\text{CH}_2\text{CH}_3)_3$  group and the nine methyl protons of the  $-\text{N}^+(\text{CH}_2\text{CH}_3)_3$  group respectively. In the case of NAH, a singlet at  $\delta$  7.11 ppm, a triplet at  $\delta$  6.86 and a singlet at  $\delta$  4.53 were observed, which were attributed to the methylene protons of the  $\text{O=CCH}_2\text{-Py}^+$  group, the amide  $-\text{HNC=O}$  proton and the methylene protons of the  $-\text{CH}_2\text{O}$ -group, respectively.

The relationship of the surface tension towards the concentration of the surfactant was investigated and illustrated in Figure 1 through the plot of the surface tension towards the log of the concentration of the surfactant. The surface tension of the surfactant was significantly determined by the chain length when the concentration was constant. Hence, low surface tension was obtained with CN-1 and CN-2 owing to their short chains. The surface tension of the surfactant absorbed on the interface of air and water increased when the chain length became longer. Nevertheless, the surface tension of various surfactants became almost the same when the concentration was high. This indicated that the surface tension of all the surfactants reached to the values of the critical micelle concentration. Overall, CN-1 exhibited the minimum critical micelle concentration, whereas NAH displayed the maximum critical micelle concentration, which suggested that the critical micelle concentration reduced when the chain length increased.

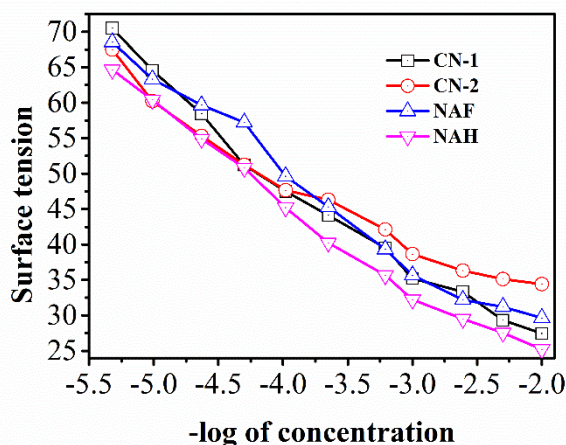


**Figure 1.** Plots of the relationship of the surface tension towards  $-\log$  of concentration of the as-synthesized surfactants.

Table 2 lists the values of the critical micelle concentrations (cmc), surface tension at the cmc ( $\gamma_{\text{cmc}}$ ),  $\Gamma_{\text{cmc}}$ , and  $A_{\text{cmc}}$  of four proposed surfactants. As expected, the surfactants give lower cmc and greater efficiency in lowering the surface tension than the monomeric surfactants. It is noteworthy that the cmc of NAH is smaller by about three orders of magnitude than that of sodium dodecanoate with

the same carboxylate headgroup. This suggests that the present NAH surfactant make it easy to form micelles in the bulk solution. The cmc of the conventional ionic surfactants is known to decrease with increasing number of carbon atoms in the hydrophobic groups up to about a hexadecyl group. In this work, the cmc of surfatants also shifts to lower concentration with increasing hydrocarbon chain length.

**Table 2.** Physicochemical properties of proposed surfactants.

Surfactant	cmc (mM/dm <sup>3</sup> )	cmc $\gamma_{cmc}$ (mN/m)	$\Gamma_{cmc}$ (M/m <sup>2</sup> )	$A_{cmc}$ (nm <sup>2</sup> /molecule)
CN-1	0.432	38.4	3.41	0.47
CN-2	0.211	30.7	3.44	0.51
NAF	0.185	28.4	3.49	0.50
NAH	0.096	28.2	3.52	0.49

The percentage inhibition efficiency (IE%) was employed to represent the corrosion inhibition performance of the as-synthesized compounds immersed in HCl with a concentration of 1.5 M, which was calculated through the equation described below:

$$IE\% = \frac{W_o - W}{W_o} \times 100$$

where the percentage inhibition efficiency was represented by IE%, and the weight loss of the carbon steel, which was immersed in HCl without and with the inhibitor, was described  $W_o$  and  $W$ , respectively.

The corrosion inhibition capacities of various as-synthesized surfactant inhibitors for the carbon steel specimens were illustrated in Table 3. The inhibition efficiency as well as the surface coverage were investigated after performing the weight loss experiment. The corrosion rate was then calculated based on the equation described below:

$$K = \frac{W}{St}$$

where  $K$  meant the corrosion rate,  $S$  and  $W$  represented the surface coverage and the mean weight loss, respectively.

Furthermore, the surface coverage was calculated based on the equation described below:

$$\Theta = 1 - \frac{W_{corr}}{W_{corr}^o}$$

where the corrosion rate of the carbon steel specimens in the presence and absence of the inhibitor were represented with  $W_{corr}$  and  $W_{corr}^o$ , respectively.

**Table 3.** Weight loss experiment of the carbon steel immersed in 1.5 M HCl in the presence and absence of various as-synthesized inhibitors.

Inhibitor	Concentration (ppm)	Corrosion rate (mg/cm <sup>2</sup> /h)	Surface coverage	Inhibition efficiency (%)
Blank	0	12.4	—	—
CN-1	50	10.51	0.152	15.2
	100	9.74	0.215	21.5
	200	8.54	0.311	31.1
	300	8.42	0.321	32.1
	500	8.12	0.345	34.5
CN-2	50	10.41	0.160	16.0
	100	9.56	0.229	22.9
	200	8.32	0.329	32.9
	300	8.17	0.341	34.1
	500	7.86	0.366	36.6
NAF	50	10.03	0.193	19.3
	100	9.25	0.254	25.4
	200	8.89	0.283	28.3
	300	8.44	0.319	31.9
	500	8.03	0.352	35.2
NAH	50	7.41	0.402	40.2
	100	8.45	0.319	31.9
	200	6.89	0.444	44.4
	300	6.29	0.505	50.5
	500	4.57	0.631	63.1

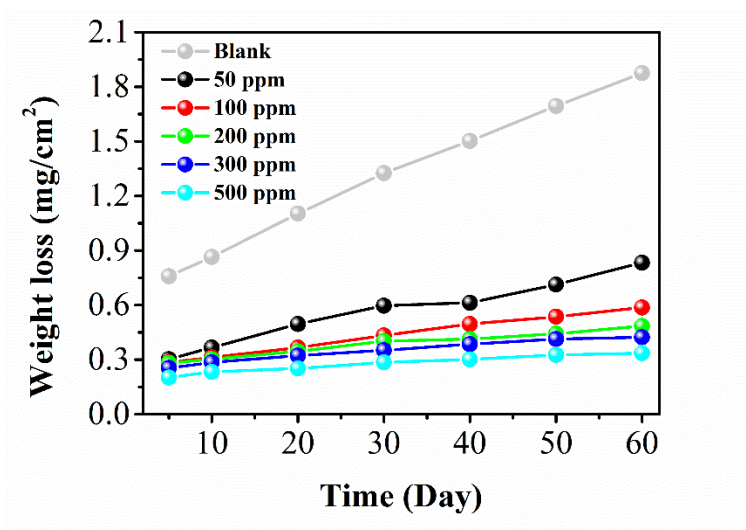


**Figure 2.** Weight loss profiles of inhibitors dipped into 1.5 M HCl for 60 days with NAH of various concentrations.

According to the results shown in Table 3, the obtained results of NAH with various concentrations were illustrated in Figure 2. It was obvious that the inhibition efficiency was enhanced significantly when increasing the concentration of NAH. A similar result has been reported by

Yıldırım et al. [12] as well. In Yıldırım's work, synthesized amide based inhibitors all exhibited very high inhibition efficiencies at high concentration condition. However, our observations suggested the inhibition efficiency performance of this series amide based inhibitors was highly related to their carbon chain length. The addition of carbon chain length could significantly improve the inhibition efficiency of the surfactant. We believe the further design the amide based surfactant by adding more carbon chains could further improve the performance. More importantly, this strategy could be used for balance of the cost and the product efficiency.

Figure 3A clarified the open circuit potentials of the carbon steel electrode which was immersed in HCl with a concentration of 1.5 M for diverse times in the presence of NAH inhibitors with various concentrations. It was obvious that the open circuit potential tended to be more negative when immersing the carbon steel electrode in HCl at the beginning, which was in accordance with the results in other reports. This was primarily induced by the protective film formed on the surface of the electrode, where the open circuit potential could be changed slightly to the positive. Moreover, the characteristic Tafel plots of the carbon steel electrode which was immersed in HCl with a concentration of 1.5 M in the presence of NAH with diverse concentrations were elaborated in Figure 3B. It was obvious that an inhibition towards the metal dissolution at the anode and the reduction reaction at the cathode took place when adding the surfactant. Besides, the inhibition performance was enhanced when increasing the concentration of NAH. The cathodic and anodic Tafel slopes of NAH with various concentrations were determined to be 488 and 282 mV/dce for 50 ppm; 259 and 213 mV/dce for 100 ppm; 208 and 206 mV/dce for 200 ppm; 316 and 193 mV/dce for 300 ppm; 361 and 211 mV/dce for 500 ppm. The shifts observed in the Tafel slopes indicated that a mixed-type inhibitors present in the system [21]. Additionally, the corrosion density decreased with the increasing concentration of the inhibitor, which suggested that the dissolution mechanism were not changed by adding inhibitor during the inhibition process to the metal dissolution at anode and the reduction reaction at cathode [22-25]. Other electrochemical corrosion parameters such as cathodic and anodic Tafel slopes, corrosion potential and corrosion current density were also obtained from polarization curves (Table 3). The result indicate the IF% performance recorded using electrochemical method is slightly higher than the results recorded in the weight loss test.

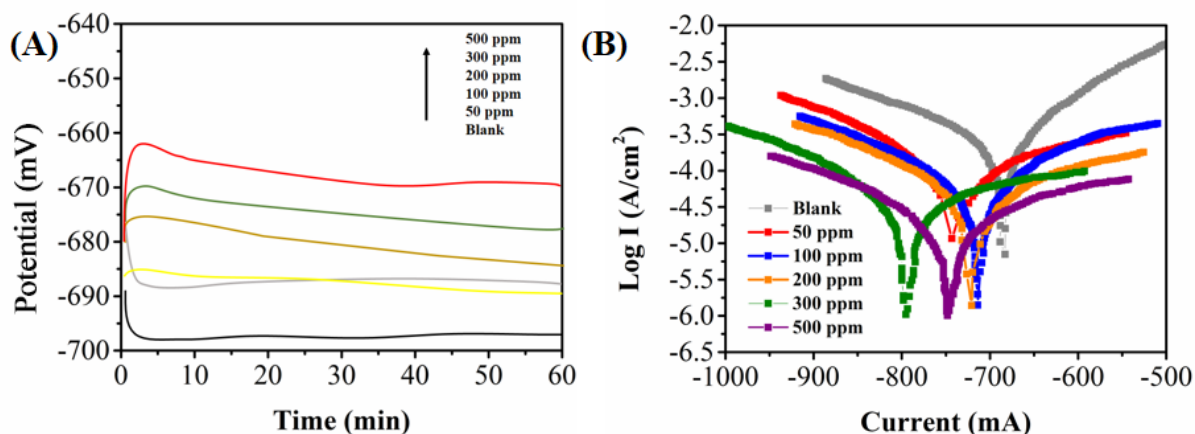


**Figure 3.** (A) Potential–time plots and (B) polarization curves of the carbon steel immersed in 1.5 M HCl with 1.



**Table 3.** Polarization parameters for carbon steel in 1.5 M HCl with different concentrations of NAH of concentrations.

NAH concentration (ppm)	Anodic slope (mV/dec)	Cathodic slope (mV/dec)	Corrosion potential (V)	corrosion density (A/cm <sup>2</sup> )	Inhibitor Efficiency (%)
50	135	145	-0.75	5.44	39.65
100	134	146	-0.73	4.65	44.58
200	149	140	-0.71	5.63	52.54
300	161	155	-0.79	5.04	63.21
500	151	152	-0.76	4.06	70.36

The Nyquist plot of the corrosion performance of the carbon steel was illustrated in Figure 4A, where the carbon steel was immersed in HCl with a concentration of 1.5 M with NAH of various concentrations. It was obvious that the impedance response of the carbon steel electrode exhibited a distinct change when NAH with various concentrations was added. Owing to the frequency dispersion effect, all the curves exhibited an inductive line when the frequency value was low, whereas a capacitive loop was observed when the frequency value was high [26]. The resistance increased when increasing the concentration of the inhibitor, which indicated that the inhibitor molecules were immobilized on the interface of the carbon steel and HCl [27]. The Bode plots of the corrosion performance of the carbon steel were illustrated in Figure 4B, where the carbon steel was immersed in HCl with a concentration of 1.5 M in the presence of NAH with various concentrations. The slopes of logZ against logf lines were calculated to be unequal to -1, which indicated that such conditions were well verified with the constant phase element [28].

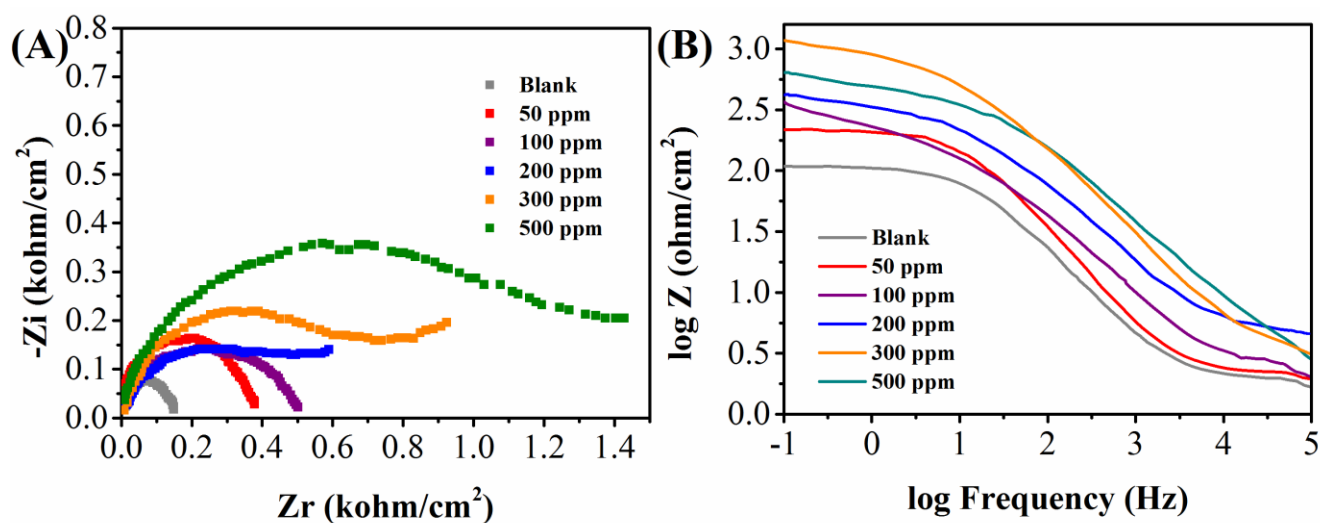


**Figure 4.** (A) Nyquist plots and (B) Bode plots of the carbon steel electrode which was dipped into 1.5 M HCl with NAH of various concentrations.

Notably, the hydrophobic part in the inhibitor molecules exhibited a significant effect on the corrosion inhibition performance of the inhibitor, as a remarkable protective layer could be formed against by the apolar interactions among the long alkyl chains in the molecules which were induced by the Van der Waals forces. Hence, for this case, the chain length became an essential factor. In general, a better corrosion inhibition performance was obtained when longer alkyl chains were employed. However, the solubility of the inhibitors reduced sometimes when the chain length was longer, resulting in the reduction of the inhibitory capacity. Besides, the inhibition could also be enhanced by the tight packing which was caused by the hydrophobic alkyl chains. These mechanisms discussed above, which were related to the corrosion inhibition effect of the as-synthesized surfactant inhibitors, were further confirmed by the measurements of the contact angle. The change of the contact angle value of the water droplet covered on the inhibitor compared to that on the free metal surface was measured to be 14.7. Moreover, the contact angles of the metal surfaces in the presence of inhibitors was measured to be 35.22, 56.21, 66.21 and 70.21, which were corresponding to CN-1, CN-2, NAF and NAH, respectively.

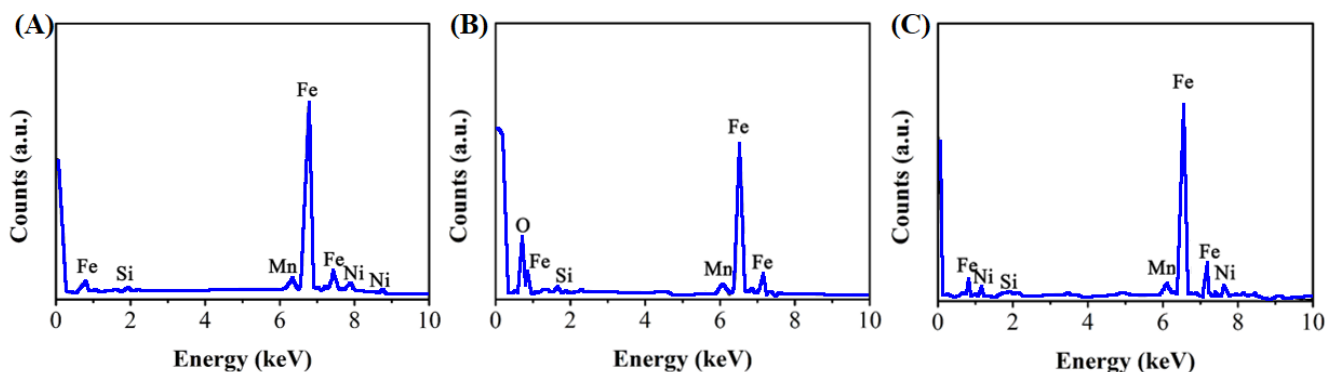


**Figure 5.** EDX images of the carbon steel samples (A) before being immersed into 1.5 M HCl, (B) after being immersed into 1.5 M HCl in the absence of any inhibitor and (C) after immersing into 1.5 M HCl in the presence of 500 ppm NAH.

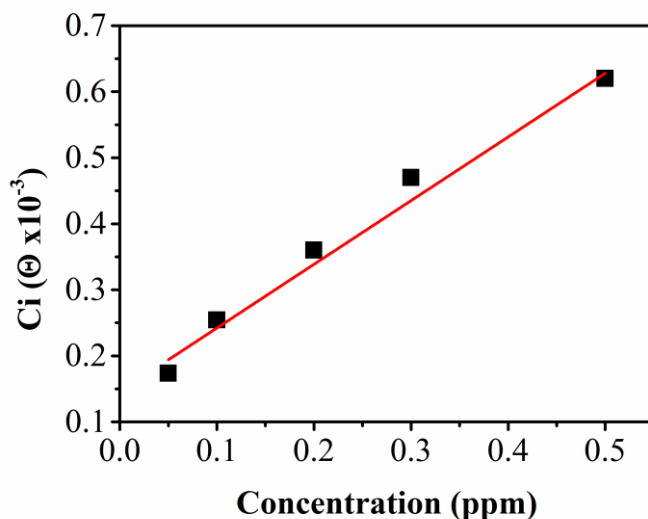


**Figure 6.** Langmuir adsorption isotherm model of NAH on the surface of the carbon steel.

A protective layer was generated on the interface between the surface of the carbon steel and 0.15 M HCl, which was confirmed by the electrochemical measurement. Then, the composition of the protective layer was analysed with energy dispersive analysis (EDX), where the Fe signal was employed to determine the thickness of the protective layer formed on the interface between the surface of the carbon steel and HCl. The EDX spectrum of the carbon steel, which was immersed in HCl with a concentration of 1.5 M in the absence of any corrosion test, was illustrated in Figure 5A. The spectrum of the carbon steel, which was placed in HCl with a concentration of 1.5 M in the absence of any inhibitor, was clarified in Figure 5B. Owing to the corrosion effect, numerous signals became weaken. By comparison, the spectrum of the carbon steel, which was immersed in 1.5 M HCl in the presence of NAH with a concentration of 500 ppm was shown in Figure 6C. In this case, owing to the protective film formed on the interface, the surface state of the carbon steel specimen was improved remarkably based on the distinct reduce of the iron band. Thus, NAH, which could be absorbed to the surface of the carbon steel specimen, exhibited remarkable inhibition efficiency [29]. According the results of the experiments described above, the inhibition effect of the inhibitor was identified by the protective layer generated on the surface of the carbon steel. Furthermore, the mode of the adsorption isotherm was investigated to be accord with the experimental results, where the surface coverage was employed to the elaboration of the adsorption isotherm as an indicator. Thereafter, Langmuir adsorption isotherm was found to completely match the experimental results. A straight line was observed in Figure 6, which indicated that the inhibition progress of the surfactant NAH was primarily induced by the interaction among the surfactant molecules absorbed on the surface of the carbon steel.

#### 4. CONCLUSIONS

In conclusion, four diverse surfactants, which contain amide group, were prepared. Various techniques were employed to determine the chemical structures and properties of the as-synthesized compounds. The performance of the four as-synthesized surfactants was evaluated on the carbon steel by HCl with a concentration of 1.5 M. The obtained results suggested that the NAH exhibited a remarkable inhibition effect, which was determined by the concentration of the NAH. Furthermore, the adsorption process of the surfactants on the surface of the carbon steel was clarified with Langmuir adsorption isotherm.

#### References

1. H.H. Hassan, E. Abdelghani and M.A. Amin, *Electrochimica Acta*, 52 (2007) 6359
2. D. Hillis, *Annals of the Rheumatic Diseases*, 69 (2014) 2131
3. X. Shi, T.A. Nguyen, Z. Suo, Y. Liu and R. Avci, *Surface & Coatings Technology*, 16 (2016) 9874
4. L.A. Schaidler, R.A. Rudel, J.M. Ackerman, S.C. Dunagan and J.G. Brody, *Science of the Total Environment*, s 468–469 (2014) 384
5. M. Ricaurte, C. Dicharry, X. Renaud and J.P. Torr e, *Fuel*, 122 (2014) 206
6. G. Han, H. Yang, X. Wang, S. Liu, R. Sun, G. Han, H. Yang, S. Liu and R. Sun, *Appl. Surf. Sci.*,

- 317 (2014) 35
7. P. Singh, A. Singh and M.A. Quraishi, *Journal of the Taiwan Institute of Chemical Engineers*, 19 (2015) 1516
  8. A. Popova, M. Christov and A. Vasilev, *Corrosion Science*, 94 (2015) 292
  9. K. Khaled and E. Ebenso, *Research on Chemical Intermediates*, 41 (2015) 49
  10. S.A. Umoren, I.B. Obot, A. Madhankumar and Z.M. Gasem, *Carbohydrate Polymers*, 124 (2015) 280
  11. L. Olasunkanmi, I.B. Obot, M.M. Kabanda and E.E. Ebenso, *Journal of Physical Chemistry C*, 119 (2015)
  12. A. Yıldırım, S. Öztürk and M. Cetin, *Journal of Surfactants and Detergents*, 16 (2013) 13
  13. D. Asefi, M. Arami, A.A. Sarabi and N.M. Mahmoodi, *Corrosion Science*, 51 (2009) 1817
  14. M.A. Hegazy, *Journal of Molecular Liquids*, 208 (2015) 227
  15. S.M. Tawfik, *Journal of Molecular Liquids*, 209 (2015) 320
  16. Z. Yan, C. Dai, M. Zhao, G. Zhao, Y. Li, X. Wu, M. Du and Y. Liu, *Colloids & Surfaces A Physicochemical & Engineering Aspects*, 482 (2015) 283
  17. S.M. Shaban, I. Aiad, H.A. Fetouh and A. Maher, *Journal of Molecular Liquids*, 212 (2015) 699
  18. S.W. Tamchang, H.A. Biebuyck, G.M. Whitesides, N. Jeon and R.G. Nuzzo, *Langmuir*, 11 (1995) 4371
  19. J.H.V. Esch, M.A.M. Hoffmann and R.J.M. Nolte, *Journal of Organic Chemistry*, 60 (1995) 1599
  20. S.A.A. El-Maksoud, *Journal of Electroanalytical Chemistry*, 565 (2004) 321
  21. P.M. Krishnegowda, V.T. Venkatesha, P.K.M. Krishnegowda and S.B. Shivayogiraju, *Ind. Eng. Chem. Res.*, 52 (2013) 722
  22. Hu, S. Hu, J. Fan, C. Jia, X. Zhang, Jun, A. Guo and Wenyue, *Acta Chimica Sinica*, 68 (2010) 2051
  23. A. Kokalj, S. Peljhan, M. Finšgar and I. Milošev, *Journal of the American Chemical Society*, 132 (2010) 16657
  24. D.M. Bastidas, M. Criado, V.M.L. Iglesia, S. Fajardo, A.L. Iglesia and J.M. Bastidas, *Cement & Concrete Composites*, 43 (2013) 31
  25. E.E. Ebenso, T. Arslan, F. Kandemirli, N. Caner and I. Love, *International Journal of Quantum Chemistry*, 110 (2010) 1003
  26. D.A. López, S.N. Simison and S.R.D. Sánchez, *Electrochimica Acta*, 48 (2003) 845
  27. U. Rammelt and G. Reinhard, *Progress in Organic Coatings*, 21 (1992) 205
  28. Müller, W. Diaternascimento, M. Luciazeddies, MiriamCórsico, MarianaGassa and L. Mabelmele, *Materials Research*, 10 (2007) 5
  29. M.A. Amin, *Journal of applied electrochemistry*, 36 (2006) 215

© 2017 The Authors. Published by ESG ([www.electrochemsci.org](http://www.electrochemsci.org)). This article is an open access article distributed under the terms and conditions of the Creative Commons Attribution license (<http://creativecommons.org/licenses/by/4.0/>).